

Heavy-flavor production and hadronization at the LHC: experimental status and perspectives from LHC experiments

Victor Feuillard^{a,*} on behalf of the ALICE, ATLAS, CMS and LHCb collaborations

^aHeidelberg University,

Im Neuenheimer Feld 226, Heidelberg, Germany

E-mail: victor.jose.gaston.feuard@cern.ch

Heavy-flavor hadrons are one of the most prominent probes to study the quark–gluon plasma and to test models based on Quantum Chromodynamics (QCD). This contribution presents the latest results regarding heavy-flavor production in ALICE, ATLAS, CMS and LHCb.

*12th Large Hadron Collider Physics Conference – LHCP 2024
3-8 June 2024
Boston, MA, US*

*Speaker

Heavy-flavor hadrons contain at least one charm or beauty valence quark. Because of the large masses of the heavy quarks, their formation time is short and, in heavy-ion collisions, they experience the whole evolution of the quark–gluon plasma (QGP) medium produced in the collision. Heavy quarks are produced in initial hard scatterings with moderate to large Q^2 and their production can be described with perturbative quantum chromodynamics (pQCD) calculations, using the factorization approach, in which the production cross-section is proportional to the parton distribution functions, the partonic cross section, and the fragmentation functions. The latter were assumed for a long time to be universal across collision systems but new results indicate otherwise.

Heavy-flavor production can be studied in several collision systems, with different goals. Measurements in proton–proton collisions allow us to test pQCD calculations describing heavy-flavor hadron production and measure the heavy-quark fragmentation functions. Measurements in proton–nucleus collisions are helpful to investigate initial-state effects such as shadowing and gluon saturation, as well as study the interplay between soft and hard processes. Finally, measurements in nucleus–nucleus collisions probe the properties of the QGP and measure the influence of final-state effects in heavy-flavor production. In the following we will present some of the latest results measured by ALICE, ATLAS, CMS and LHCb on heavy-flavor production and hadronization.

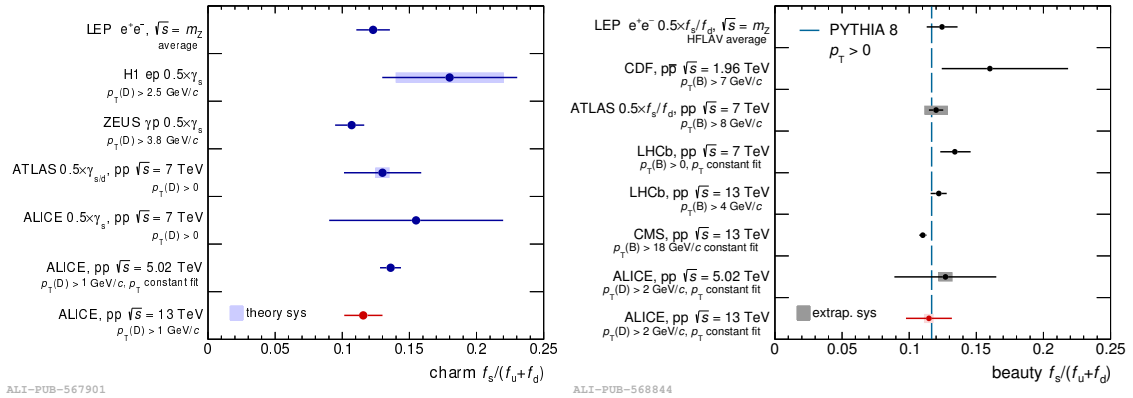


Figure 1: Left: Ratio of strange-to-non-strange charm fragmentation functions measured by ALICE in pp collisions at $\sqrt{s} = 13$ TeV compared with other experiments [1]. Right: Ratio of strange-to-non-strange beauty fragmentation functions measured by ALICE in pp collisions at $\sqrt{s} = 13$ TeV compared with other experiments [2].

The production of prompt and non-prompt D mesons has been measured by ALICE in pp collisions at $\sqrt{s} = 13$ TeV [1, 2]. The strange-to-non-strange production yield ratio, $D_s^+/(D^0 + D^+)$, has been measured as a function of p_T . In the prompt case, the ratio exhibits an increasing trend as a function of p_T up to around 8 GeV/c, while no significant trend is visible in the non-prompt case due to the larger uncertainties. The non-prompt measurement has been compared with FONLL pQCD calculations [3], which are able to describe the data in the whole p_T range. From these measurements the strange-to-non-strange ratio of fragmentation functions can be extracted. The corresponding result is presented in Figure 1 for the charm (left) and beauty (right) cases, and compared with measurements by other experiments and in other collision systems. All measurements are in

agreement within uncertainties, indicating a universality of the relative fragmentation function for charm and beauty mesons.

The strange-to-non-strange production yield ratio for beauty has also been measured in Pb–Pb collisions for the B mesons by CMS [4] and non-prompt D mesons by ALICE [5–7]. These results show a hint that strange mesons are less suppressed than non-strange mesons, as is expected in the presence of strangeness enhancement inside a QGP. A transport model implementing strangeness enhancement and hadronization via recombination [8] is compatible with data, as well as predictions from a statistical hadronization model [9]. However, due to the large uncertainties on the data, the measurements are also compatible with a scenario without strangeness enhancement.

The Λ_c^+ -baryon production has been measured at mid-rapidity by CMS in pp collisions at $\sqrt{s} = 5.02$ TeV [10] and ALICE in pp collisions at $\sqrt{s} = 13$ TeV [11] for $p_T > 3$ GeV/c and $p_T > 1$ GeV/c, respectively. The Λ_c^+ over D^0 yield ratio is presented in Figure 2, compared with earlier measurements of the Λ_b^+ over B ratio from LHCb [12] at forward rapidity.

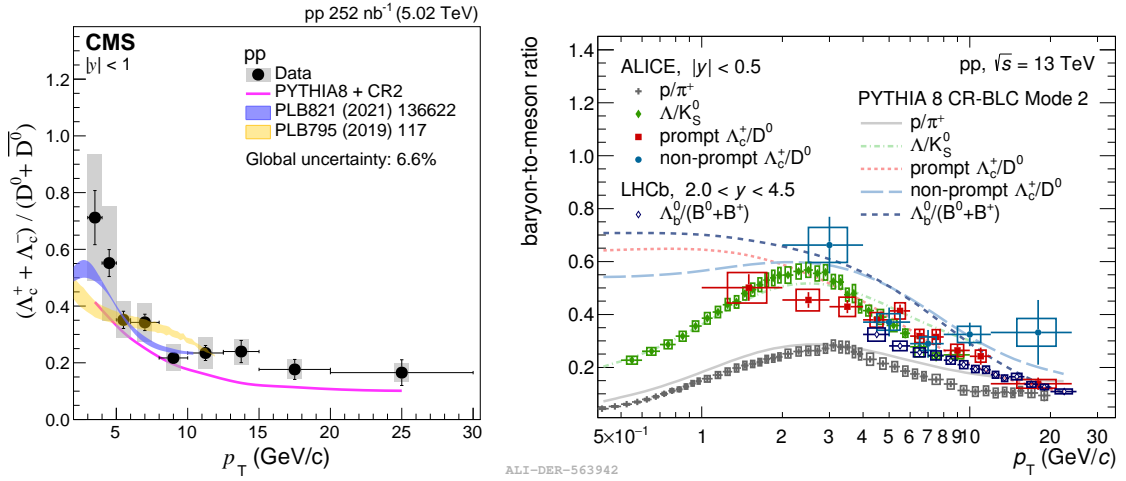


Figure 2: Left: Prompt and non-prompt Λ_c^+ over D^0 production yield ratio measured by CMS in pp collisions at $\sqrt{s} = 5.02$ TeV [10] compared with different models [13–15]. Right: Λ_c^+ over D^0 production ratio measured by ALICE in pp collisions at $\sqrt{s} = 13$ TeV [11] compared with PYTHIA calculations [13] and LHCb measurements of the Λ_b^+ /B yield ratio [12].

In both CMS and ALICE, the Λ_c^+ over D^0 production ratio shows a decreasing trend with increasing p_T , differently from what was measured in leptonic collisions, where no significant p_T dependence was observed. PYTHIA8 [13] calculations implementing a specific tune with color reconnection beyond leading color (BLC-CR mode 2) show a good agreement with the data. The non-prompt Λ_c^+ over D^0 ratio measured by ALICE is generally higher than the Λ_b^+ over B ratio measured by LHCb. Models with coalescence and fragmentation processes [14] show a good agreement in the available p_T range and reproduce the decreasing trend over p_T . The statistical hadronization model [15] also shows a good agreement with the data in the available p_T range.

These measurements are extended to additional states by new results coming from Run 3 of the LHC, as illustrated by the first measurement of the $\Sigma_c^{0,++}(2520)$ in ALICE presented in Figure 3. The $\Sigma_c^{0,++}(2520)/\Sigma_c^{0,++}(2455)$ ratio is consistent with the p_T -integrated result from e^+e^-

collisions within the uncertainties in the investigated p_T region. The result is compared with several calculations: PYTHIA 8 [16] Monash overestimates the data, while the CR Modes underestimate the data. The Statistical Hadronization Model [17] prediction also slightly underestimates the data in the common p_T range.

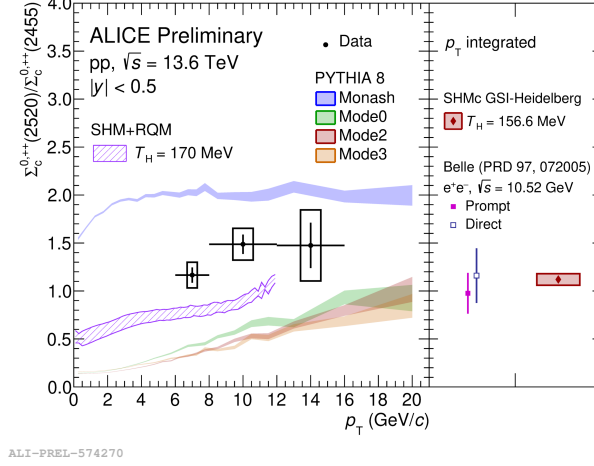


Figure 3: Measurement of the $\Sigma_c^{0,++}(2520)/\Sigma_c^{0,++}(2455)$ yield ratio in ALICE compared with models [16–18] and Belle measurement [19].

The Ξ_c^+/D^0 and Ξ_c^+/Λ_c^+ production yield ratios have been measured in p–Pb collisions by ALICE at $\sqrt{s_{NN}} = 5.02$ TeV [20] and by LHCb at $\sqrt{s_{NN}} = 8.16$ TeV [21]. The results are presented in Figure 4.

The results from ALICE and LHCb are compatible within the uncertainties, although the ALICE result tend to be higher. The ratios show no significant p_T dependence for both p-going and Pb-going directions in both ALICE and LHCb, which is a strong indication that the same processes govern hadronization in forward and backward rapidity. The LHCb data are also compared with models (Figure 4 right). The EPPS16 [23] predictions overestimate the LHCb data but show a similar trend, while agreeing with the ALICE measurements. PYTHIA8.3 BLC-CR mode 2 [13] calculations lie on the lower edge of the data uncertainties, and EPOS4HQ [24] calculations describe the data but show a different trend as a function of p_T with respect to the LHCb measurement.

All the measurements of heavy-flavor mesons and baryons were used to evaluate the charm fragmentation fractions [25], which are shown in Figure 5. The values obtained by ALICE are consistent between pp and p–Pb collisions. However a large difference is observed with respect to e^+e^- and ep collisions: an increase in the Λ_c^+ production is accompanied by a concomitant decrease in non-strange D-meson production. This indicates that the universality of parton-to-hadron fragmentation is not generally valid, contrary to what was assumed until now.

The ATLAS experiment has measured the two-muon correlation functions in pp collisions at $\sqrt{s} = 5.02$ TeV and Pb–Pb collisions at $\sqrt{s_{NN}} = 5.02$ TeV as a function of the azimuthal angle difference $\Delta\phi$ [26]. As expected for semileptonic decays of heavy-quark pairs, a strong peak is visible at $\Delta\phi = \pi$, with a width that can be quantified by a FWHM Γ or a standard deviation σ , on top of an uncorrelated pedestal. The peak widths are shown in Figure 6, and are the same for

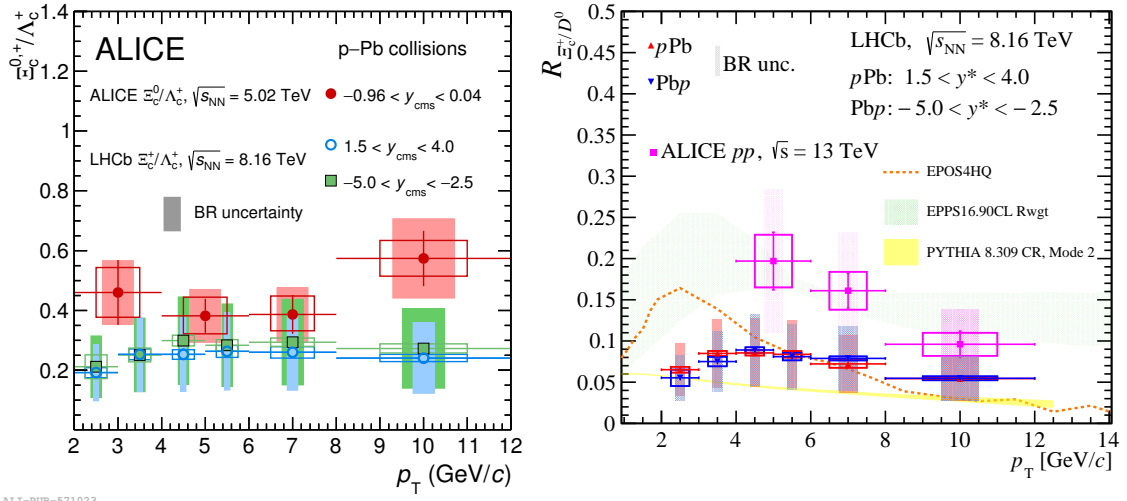


Figure 4: Left: Ξ_c^+/Λ_c^+ ratio measured by ALICE at $\sqrt{s_{NN}} = 5.02$ TeV [20] and LHCb at $\sqrt{s_{NN}} = 8.16$ TeV [21] Right: Ξ_c^+/D^0 ratio measured LHCb at $\sqrt{s_{NN}} = 8.16$ TeV [21] compared with ALICE measurements in pp collisions [22] and EPSS16 [23], PYTHIA [13] and EPOS [24] predictions.

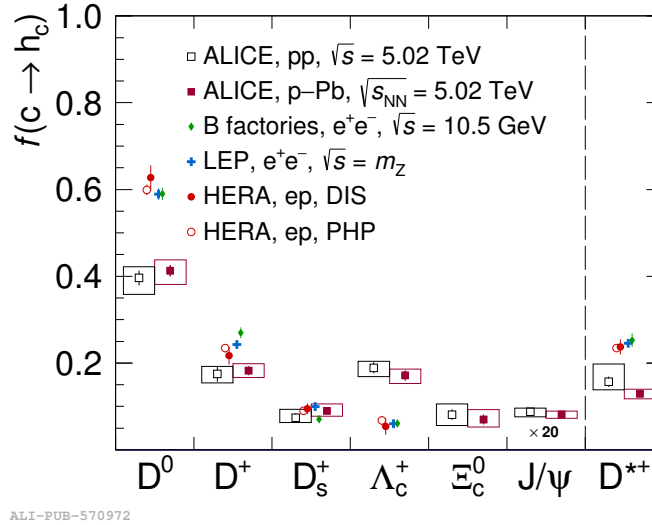


Figure 5: Charm fragmentation fraction measured by ALICE in pp and p-Pb collisions compared with other collision systems [25].

the same-sign and opposite-sign pairs, indicating a dominance of beauty decays in this kinematic region. The widths in Pb-Pb collisions are the same as in pp collisions, except for the most central collisions, which show a narrower peak. This could be an effect of a different p_T distribution of the originating b quarks, which is modified by the energy loss of the quarks in the QGP, but does not support the predicted systematic increase in the Γ broadening from peripheral to central collisions

due to interactions in the QGP [27]. The bottom panel of Figure 6 shows that the square of such an additional broadening in Pb–Pb collisions with respect to pp collisions is negligible and even results in a negative contribution at 90% confidence level in the most central interval.

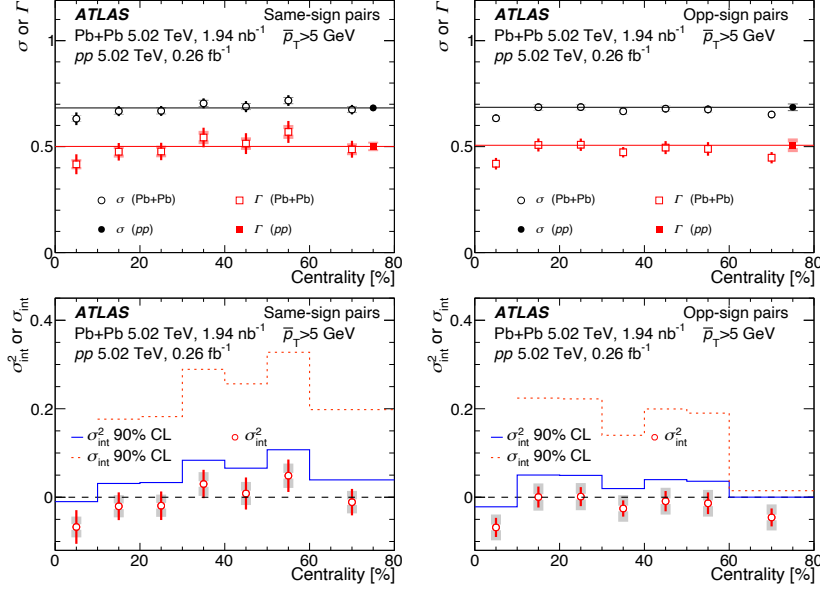


Figure 6: Two-muon correlation function peak widths as a function of centrality, in pp and Pb–Pb collisions at $\sqrt{s_{\text{NN}}} = 5.02$ TeV [26].

Finally, the $J/\psi/D^0$ ratio has been measured by ALICE in Pb–Pb collisions at $\sqrt{s_{\text{NN}}} = 5.02$ TeV [28]. This ratio provides a tight constraint to models because it simultaneously describes open and hidden charm production using only the measured charm production cross-section, and is particularly sensitive to the hadronization mechanisms of the different charm hadrons. The result is presented in Figure 7 as a function of centrality compared with SHMc model predictions [18]. The ratio is higher in most central collision interval, a feature correctly described by the SHMc model. This hints that both J/ψ and D^0 are produced via the statistical hadronization of deconfined and locally thermalized charm quarks.

In conclusion, the presented results show that the measurement of multiple heavy-flavor species offers a solid ground to test pQCD models and the factorization approach, and suggests a breaking of universal hadronization across different collision systems. The ability to measure several observables (R_{AA} , production ratios...) provides many avenues for model comparison and improves our understanding of heavy-quark interaction with the medium. Measurements indicate that, in Pb–Pb collisions, charm hadrons can also be produced through coalescence or statistical recombination at low and moderate p_{T} , whereas no significant contribution from coalescence is observed at high p_{T} in Pb–Pb collisions. With new results coming out of the ongoing Run 3 of the LHC, more precise measurements with reduced uncertainties will be able to further improve our understanding of heavy-flavor production and hadronization.

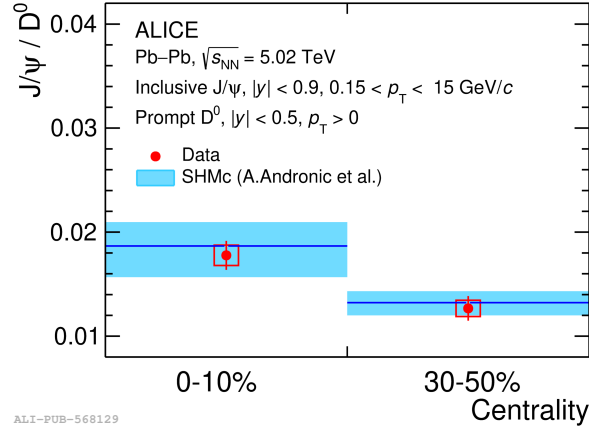


Figure 7: $J/\psi/D^0$ ratio as a function of centrality in Pb–Pb collisions at $\sqrt{s_{\text{NN}}} = 5.02$ TeV [28] compared with SHMc predictions [18].

References

- [1] ALICE Collaboration, *JHEP* **12** (2023) 086 [2308.04877].
- [2] ALICE Collaboration, *JHEP* **10** (2024) 110 [2402.16417].
- [3] M. Cacciari et al., *JHEP* **10** (2012) 137 [1205.6344].
- [4] CMS Collaboration, *Phys. Lett. B* **829** (2022) 137062 [2109.01908].
- [5] ALICE Collaboration, *Phys. Lett. B* **846** (2023) 137561 [2204.10386].
- [6] ALICE Collaboration, *Phys. Lett. B* **827** (2022) 136986 [2110.10006].
- [7] ALICE Collaboration, *JHEP* **01** (2022) 174 [2110.09420].
- [8] M. He, R.J. Fries and R. Rapp, *Phys. Lett. B* **735** (2014) 445 [1401.3817].
- [9] P. Braun-Munzinger, K. Redlich, N. Sharma and J. Stachel, 2408.07496.
- [10] CMS Collaboration, *JHEP* **01** (2024) 128 [2307.11186].
- [11] ALICE Collaboration, *Phys. Rev. D* **108** (2023) 112003 [2308.04873].
- [12] LHCb Collaboration, *Phys. Rev. D* **100** (2019) 031102 [1902.06794].
- [13] J.R. Christiansen and P.Z. Skands, *JHEP* **08** (2015) 003 [1505.01681].
- [14] V. Minissale, S. Plumari and V. Greco, *Phys. Lett. B* **821** (2021) 136622 [2012.12001].
- [15] M. He and R. Rapp, *Phys. Lett. B* **795** (2019) 117 [1902.08889].
- [16] J.R. Christiansen and P.Z. Skands, *JHEP* **08** (2015) 003 [1505.01681].
- [17] M. He and R. Rapp, *Phys. Lett. B* **795** (2019) 117 [1902.08889].
- [18] A. Andronic, P. Braun-Munzinger, M.K. Köhler, K. Redlich and J. Stachel, *Phys. Lett. B* **797** (2019) 134836 [1901.09200].
- [19] Belle Collaboration, *Phys. Rev. D* **97** (2018) 072005 [1706.06791].
- [20] ALICE Collaboration, 2405.14538.
- [21] LHCb Collaboration, *Phys. Rev. C* **109** (2024) 044901 [2305.06711].
- [22] ALICE Collaboration, *Phys. Rev. Lett.* **127** (2021) 272001 [2105.05187].
- [23] K.J. Eskola, P. Paakkinen, H. Paukkunen and C.A. Salgado, *Eur. Phys. J. C* **77** (2017) 163 [1612.05741].
- [24] K. Werner and B. Guiot, *Phys. Rev. C* **108** (2023) 034904 [2306.02396].
- [25] ALICE Collaboration, 2405.14571.
- [26] ATLAS Collaboration, *Phys. Rev. Lett.* **132** (2024) 202301 [2308.16652].
- [27] M. Nahrgang, J. Aichelin, P.B. Gossiaux and K. Werner, *Phys. Rev. C* **90** (2014) 024907 [1305.3823].
- [28] ALICE Collaboration, *Phys. Lett. B* **849** (2024) 138451 [2303.13361].